AMERICAN SOCIETY FOR MICROBIOLOGY | Applied and Environmental Microbiology®

ENVIRONMENTAL MICROBIOLOGY

Molecular Determinants of the Thickened Matrix in a Dual-Species *Pseudomonas aeruginosa* and *Enterococcus faecalis* Biofilm

Keehoon Lee,[a,b] Kang-Mu Lee,[a] Donggeun Kim,[a,b] Sang Sun Yoon[a,b,c]

Department of Microbiology and Immunology,[a] Brain Korea 21 PLUS Project for Medical Sciences,[b] and Institute for Immunology and Immunological Diseases,[c] Yonsei University College of Medicine, Seoul, South Korea

ABSTRACT Biofilms are microbial communities that inhabit various surfaces and are surrounded by extracellular matrices (ECMs). Clinical microbiologists have shown that the majority of chronic infections are caused by biofilms, following the introduction of the first biofilm infection model by J. W. Costerton and colleagues (J. Lam, R. Chan, K. Lam, and J. W. Costerton, Infect Immun 28:546–556, 1980). However, treatments for chronic biofilm infections are still limited to surgical removal of the infected sites. *Pseudomonas aeruginosa* and *Enterococcus faecalis* are two frequently identified bacterial species in biofilm infections; nevertheless, the interactions between these two species, especially during biofilm growth, are not clearly understood. In this study, we observed phenotypic changes in a dual-species biofilm of *P. aeruginosa* and *E. faecalis*, including a dramatic increase in biofilm matrix thickness. For clear elucidation of the spatial distribution of the dual-species biofilm, *P. aeruginosa* and *E. faecalis* were labeled with red and green fluorescence, respectively. *E. faecalis* was located at the lower part of the dual-species biofilm, while *P. aeruginosa* developed a structured biofilm on the upper part. Mutants with altered exopolysaccharide (EPS) productions were constructed in order to determine the molecular basis for the synergistic effect of the dual-species biofilm. Increased biofilm matrix thickness was associated with EPSs, not extracellular DNA. In particular, Pel and Psl contributed to interspecies and intraspecies interactions, respectively, in the dual-species *P. aeruginosa* and *E. faecalis* biofilm. Accordingly, targeting Pel and Psl might be an effective part of eradicating *P. aeruginosa* polymicrobial biofilms.

IMPORTANCE Chronic infection is a serious problem in the medical field. Scientists have observed that chronic infections are closely associated with biofilms, and the vast majority of infection-causing biofilms are polymicrobial. Many studies have reported that microbes in polymicrobial biofilms interact with each other and that the bacterial interactions result in elevated virulence, in terms of factors, such as infectivity and antibiotic resistance. *Pseudomonas aeruginosa* and *Enterococcus faecalis* are frequently isolated pathogens in chronic biofilm infections. Nevertheless, while both bacteria are known to be agents of numerous nosocomial infections and can cause serious diseases, interactions between the bacteria in biofilms have rarely been examined. In this investigation, we aimed to characterize *P. aeruginosa* and *E. faecalis* dual-species biofilms and to determine the molecular factors that cause synergistic effects, especially on the matrix thickening of the biofilm. We suspect that our findings will contribute to the development of more efficient methods for eradicating polymicrobial biofilm infections.

KEYWORDS *Enterococcus faecalis*, *Pseudomonas aeruginosa*, biofilms, polymicrobial

Received 26 May 2017 **Accepted** 15 August 2017

Accepted manuscript posted online 25 August 2017

Citation Lee K, Lee K-M, Kim D, Yoon SS. 2017. Molecular determinants of the thickened matrix in a dual-species *Pseudomonas aeruginosa* and *Enterococcus faecalis* biofilm. Appl Environ Microbiol 83:e01182-17. https://doi.org/10.1128/AEM.01182-17.

Editor Hideaki Nojiri, University of Tokyo

Address correspondence to Sang Sun Yoon, sangsun_yoon@yuhs.ac.

Biofilms are communities of microbes that dwell on surfaces and are surrounded by extracellular matrices (ECMs) (1). The major characteristics of biofilms are high resistance to antibiotics and other various stresses, a high rate of horizontal gene transfer (HGT), and differential gene expression patterns relative to the planktonic state (1). Biofilms became a popular concept in microbiology approximately 3 decades ago; however, microbiologists still face many difficulties in studying and managing biofilms. Biofilms exist on most surfaces and cause serious problems in the medical field as infectious agents and reservoirs for many pathogens (2, 3). Chronic infections are caused by bacteria in a biofilm mode of growth (3). Due to biofilm characteristics, chronic biofilm infections are very difficult to eradicate (4). There are two major categories of biofilm infection: those associated with medically implanted devices (5–9), and those directly associated with tissues, such as chronic otitis media, dental plaque, endocarditis, lung infections in cystic fibrosis patients, urinary tract infections, and chronic wound infections (4, 10–13). The vast majority of biofilm infections contain more than one species of bacterium, fungus, or other microbe (13).

Several studies have investigated polymicrobial biofilms and have identified beneficial and synergistic interactions between microbes in a biofilm. The interactions in a polymicrobial biofilm affect its overall function, physiology, or surroundings, which enhance resistance or virulence (10, 13, 14). For example, many microbes exist in dental plaque and undergo spatiotemporal interactions, wherein one bacterial species attaches to the tooth surface and alters the surroundings to fit the next bacterial species (15). *Staphylococcus aureus* has been shown to increase infectivity, biofilm development, and antibiotic resistance when grown with *Candida albicans* in serum (14). Also, *Pseudomonas aeruginosa* has been shown to enhance virulence when incubated with Gram-positive bacteria (16).

Pseudomonas species are Gram-negative bacilli and are ubiquitous in the environment; some cause disease in both animals and plants. Among the *Pseudomonas* species, *Pseudomonas aeruginosa* is a common human opportunistic pathogen and can cause serious infections. *P. aeruginosa* is also a very common causative agent of health care-associated infections (HAIs) and the second most common cause of ventilator-associated pneumonia (VAP) in the United States. *P. aeruginosa* is known to produce various virulence factors, and the expression of these virulence factors is regulated by complex signal transduction systems in response to changes in the surrounding environment, such as biofilm formation (17).

Enterococci are Gram-positive cocci and opportunistic pathogens that are frequently isolated in the normal flora of the human gastrointestinal tract, oral cavity, and female genital tract. Enterococci have been reported to readily adhere to various medical devices and produce biofilms (18). Among enterococcal species, *Enterococcus faecalis* is the most common nosocomial pathogen and typically causes urinary tract infections, peritonitis, bacteremia, infections in abscesses, decubiti, and foot ulcers, and endocarditis. The pathogen is responsible for approximately 90% of all enterococcus-related HAIs (18–20). Furthermore, because of its ability to resist various antibiotics, *E. faecalis* causes serious problems in clinical areas (21).

P. aeruginosa and *E. faecalis* share many characteristics and niches and have been found together in clinical samples from humans (9, 15, 20). Even though several studies have investigated synergism in polymicrobial biofilms, only a few studies on polymicrobial biofilms with *P. aeruginosa* and *E. faecalis* have been undertaken. For instance, there is evidence that *P. aeruginosa* uses peptidoglycan molecules of Gram-positive bacteria as a signal to produce more virulence factors and antimicrobials, which damages the host and alters the microbiome compositions (22). Also, a study showed that pyelonephritis caused by *P. aeruginosa* was exacerbated by coinfection with *E. faecalis* (23). In the present research, synergistic effects of biofilm development were detected, including enhanced matrix thickness in *P. aeruginosa* and *E. faecalis* dual-species biofilms. Since this synergistic effect of the dual-species biofilm might enhance its virulence, the molecular elements for the synergistic effects were investigated. In order to investigate the dual-species biofilm, we constructed mutants with altered

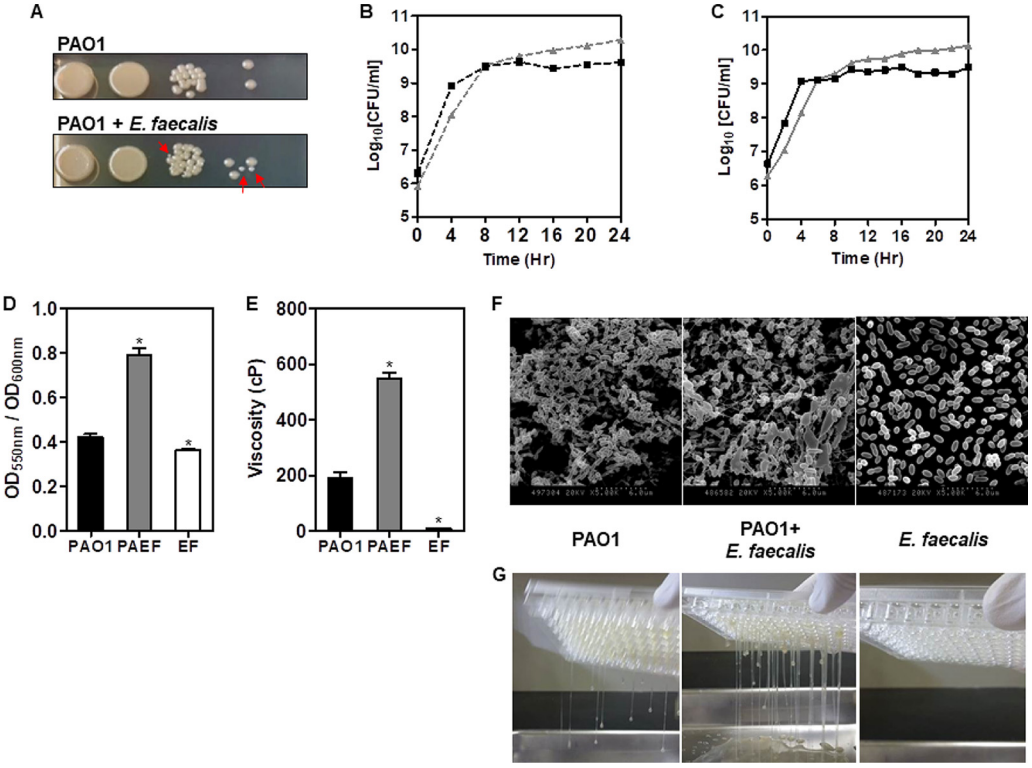

FIG 1 Polymicrobial biofilm tests of *P. aeruginosa* and *E. faecalis*. (A) Colony observation of cocultured *P. aeruginosa* and *E. faecalis* (red arrows). The growth experiment of *P. aeruginosa* (gray triangle) and *E. faecalis* (black square), grown individually (B) or together (C), in a shaking incubator at 37°C. The viable count assay was used to determine the CFU per milliliter. (D) The CV biofilm assay of the monospecies and the dual-species biofilms. *, $P < 0.001$ versus the biofilm levels of PAO1 and PAO1 plus *E. faecalis* (PAEF) or *E. faecalis* (EF). (E) Viscosity measurements of the mono- and dual-species biofilms. Viscosity appears in units of centipoise (cP). *, $P < 0.0001$ versus viscosity of PAO1 and PAEF or EF. (F) SEM images of the mono- and dual-species biofilms of *P. aeruginosa* and/or *E. faecalis*. The magnifications are ×5,000. (G) Images of the mono- and dual-species biofilms of *P. aeruginosa* and/or *E. faecalis* dripping out of the 96-well plates. Detailed video clips are provided in the movies in the supplemental material.

exopolysaccharide (EPS) production and several fluorescent strains. We also described the characteristics of the dual-species *P. aeruginosa* and *E. faecalis* biofilm using various techniques, such as viscosity measurement, a crystal violet assay, and confocal laser scanning microscopy. In light of our results, we suggest that the increased matrix thickness of the dual-species biofilm was due, in part, to the expression of Pel and Psl EPSs by *P. aeruginosa*. In conclusion, we suggest a simple model for dual-species *P. aeruginosa* and *E. faecalis* biofilm development and possible molecules that could be targeted for more effective eradication of *P. aeruginosa* polymicrobial biofilm infections.

RESULTS

Coculture and biofilm development of *P. aeruginosa* and *E. faecalis*. Wild-type *P. aeruginosa* PAO1 and *E. faecalis* were grown together in brain heart infusion broth (BHIB) medium. Each bacterial species was differentiated via colony morphology (Fig. 1A). Planktonic growth experiments of individual bacterial samples and cocultured samples were conducted to determine if one bacterial species affected the growth of the other bacterial species. The CFU per milliliter values were used to plot the data in lieu of optical density, due to interference from the excessive production of extracellular materials (Fig. 1B and C). Each bacterial species presented very similar growth patterns and generated similar numbers of bacterial cells during growth (Fig. 1B). Cocultured samples presented a growth pattern almost identical to that of individually grown cultures (Fig. 1C). The results of the growth experiment indicated that *P. aeruginosa* and *E. faecalis* did not affect each other during planktonic growth.

Dual-species biofilm development with *P. aeruginosa* and *E. faecalis* was conducted to determine if interactions occur between the two bacterial species during biofilm development. First, the amount of biofilm formation was measured using the standard crystal violet (CV) assay (Fig. 1D). The data indicated that the dual-species biofilm showed enhanced biofilm formation compared to the monospecies biofilms (Fig. 1D). During biofilm development, an interesting biofilm phenotype was observed. The biofilm exhibited a highly sticky phenotype when the two bacterial species were incubated together (see the movies in the supplemental material). Thus, the viscosities of the biofilms were measured using a viscosity meter, revealing a significantly higher viscosity for the dual-species biofilm than for the monospecies biofilms (Fig. 1E). Scanning electron microscope (SEM) images also revealed corresponding biofilm phenotypes (Fig. 1F). The SEM images of *P. aeruginosa* biofilms showed ECMs with encased and connected bacterial cells, whereas the *E. faecalis* biofilm SEM images showed no ECMs, with barely any structures. The dual-species biofilm, however, revealed significantly greater amounts of ECM than connected cells of both the same and different species. The images of the corresponding biofilms dripping out of the 96-well plates are displayed in Fig. 1G and Movie S1. The images demonstrate a stickier phenotype of the dual-species biofilm than the monospecies biofilms.

Spatial composition of the dual-species biofilm. It is very important to distinguish bacterial strains in polymicrobial biofilm investigation in order to determine the accurate distribution of each species in the biofilm architecture. To distinguish *P. aeruginosa* and *E. faecalis* under confocal laser scanning microscope (CLSM), each bacterium was inserted with different fluorescent plasmids: pME-dsRED for *P. aeruginosa*, and pMV158GFP for *E. faecalis*. Both bacterial strains harboring recombinant fluorescence plasmids were incubated in appropriate medium, with BHIB, gentamicin (5 μg/ml), and tetracycline (1 μg/ml), to prevent the loss of plasmids during growth; the medium did not affect the growth or biofilm formation of the bacteria (data not shown). Both monospecies bacterial cultures presented fluorescence, with red for *P. aeruginosa* pME-dsRED (PAO1/red) and green for *E. faecalis* pMV158GFP (*EF*/green) (Fig. S2A and B). The two bacterial species were clearly distinguishable in the dual-species culture (Fig. S2C). Growth experiments were conducted to confirm that the growth pattern was the same as that with strains lacking fluorescence constructs. The results showed that fluorescent bacteria had growth patterns identical to those of nonfluorescent bacteria (Fig. S3A to C) and that the biofilm development pattern was also identical (Fig. S3D).

The biofilms of PAO1/red and *EF*/green were analyzed by CLSM and ImageJ program analyses. The Z-stack images of each biofilm were captured by CLSM, and the fluorescence intensities of each focal plane were analyzed using ImageJ (Fig. 2). Biofilm in CLSM observations disappeared around a relative fluorescence intensity of 13 in all biofilm samples. Thus, the relative fluorescence intensity of 13 was considered the threshold for biofilm detection. The CLSM images revealed a flat PAO1/red biofilm with a height of 103 μm (Fig. 2A, bottom view). Fluorescence intensity demonstrated that most of the biofilm could be detected around 15 to 20 μm, gradually decreasing thereafter (Fig. 2A). The *EF/*green biofilm also exhibited a flat biofilm, although the height of the biofilm was around 50 μm (Fig. 2C, bottom view), much thinner than the PAO1/red biofilm. In addition, the fluorescence intensity decreased more rapidly than in the PAO1/red biofilm (Fig. 2C). The dual-species biofilm exhibited a striking difference in the spatial distribution of each species along the height of the biofilm. The Z-stack images showed a flat *EF/*green biofilm at the bottom of the polymicrobial biofilm with a cluster-structured biofilm of PAO1/red on top of it. The fluorescence intensity measurements showed a stronger *EF/*green fluorescence relative to PAO1/red fluorescence at or below the height of 30 μm, with the PAO1/red fluorescence intensity more dominant than the *EF/*green at planes higher than 30 μm (Fig. 2B).

Effect of extracellular DNA on biofilm development. The dual-species PAO1 and *E. faecalis* biofilm produced a significantly thicker matrix that was not detected in

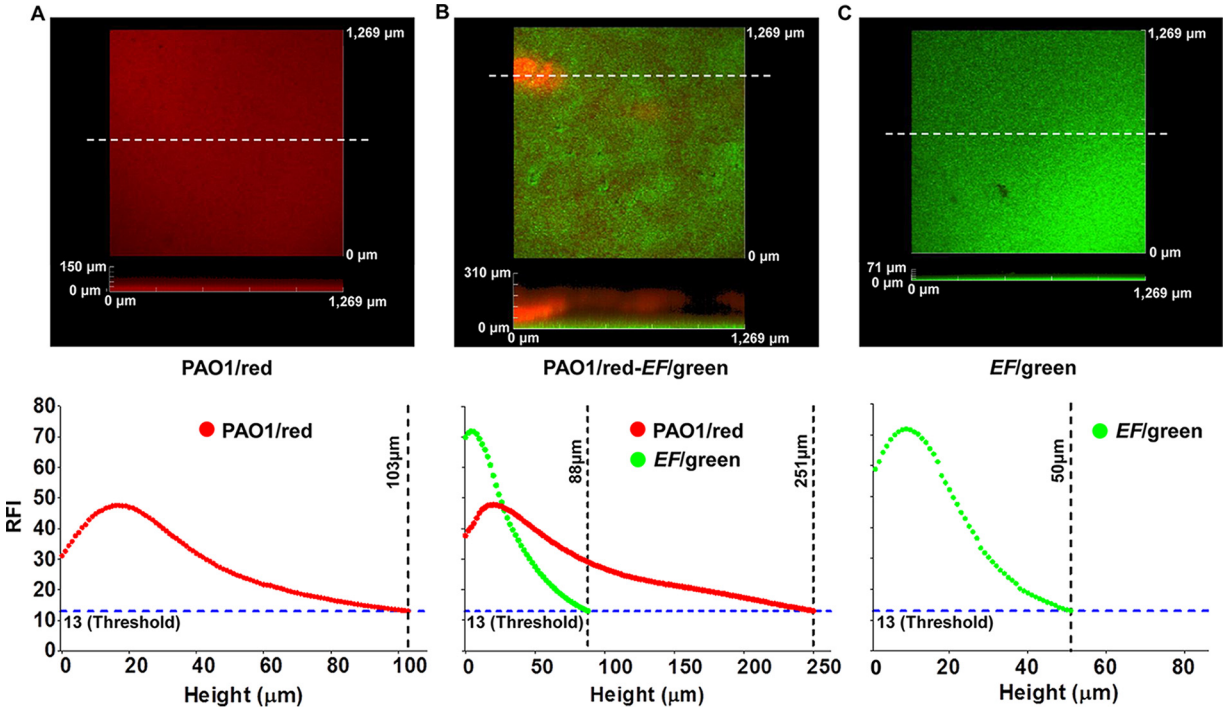

FIG 2 CLSM image analysis of mono- and dual-species PAO1/red and *EF*/green biofilms. CLSM images and their relative fluorescent intensity measures along the heights of biofilms of PAO1/red (A), PAO1/red and *EF*/green (B), and *EF*/green (C). White dotted lines indicate the locations of sagittal sections for height representation of the biofilms. The relative fluorescence intensity (RFI) of 13 was considered the threshold for biofilm detection. The biofilms were incubated at 37°C for 48 h. The relative fluorescence intensities were measured using the ImageJ program.

monospecies biofilms (Fig. 1E). In order to determine which component of the ECM contributed to the enhancement of matrix thickness in the dual-species biofilm, we sought to assess the presence of extracellular DNA (eDNA), which has been determined to be a major ECM component (24, 25). To achieve this goal, we stained biofilms with TOTO-1, a DNA-specific green fluorescent dye that does not penetrate live bacterial cells. Green fluorescent signals were not detected in the *E. faecalis* monospecies biofilm, demonstrating that no eDNA was present inside the biofilm (Fig. 3A and S4A). In contrast, strong fluorescent signals were detected in the PAO1 monospecies biofilm (Fig. 3B and S4B). Of note, a slightly lower level of eDNA-specific signaling was observed in the dual-species biofilm (Fig. 3C and S4C). Images revealed that *E. faecalis* biofilm produced very small amounts of eDNA. On the other hand, PAO1 produced large amounts of eDNA in its biofilm. The dual-species biofilm presented larger amounts of eDNA than the mono-*E. faecalis* biofilm but smaller amounts than the mono-PAO1 biofilm (Fig. S4). Furthermore, a CV biofilm assay indicated that the biofilm integrity was not affected when 32-h-old mature biofilms were treated with DNase I for 2 h (Fig. 3D). These results suggest that eDNA is not likely responsible for the matrix thickening in the dual-species biofilm.

Effects of *P. aeruginosa* EPSs on the formation of the thicker matrix of the dual-species biofilm. We next examined whether the matrix thickening of the dual-species biofilm is caused by overproduction of EPS molecules. First, we tested the role of alginate, an EPS molecule produced by mucoid *P. aeruginosa* strains (26). Although alginate is not a major component of nonmucoid PAO1 biofilms (27), we postulated that alginate production might be stimulated during dual-species biofilm formation. An alginate-negative PAO1 mutant, the Δ*alg* mutant, displayed levels of biofilm matrix thickening comparable to that of the PAO1 biofilm when it formed a monospecies biofilm (Fig. 4A and Movie S2). Importantly, the dual-species biofilm of the Δ*alg* mutant plus *E. faecalis* presented the same matrix thickness as that observed in the PAO1 plus *E. faecalis* biofilms (Fig. 4B and Movie S3). These results suggest that alginate has no

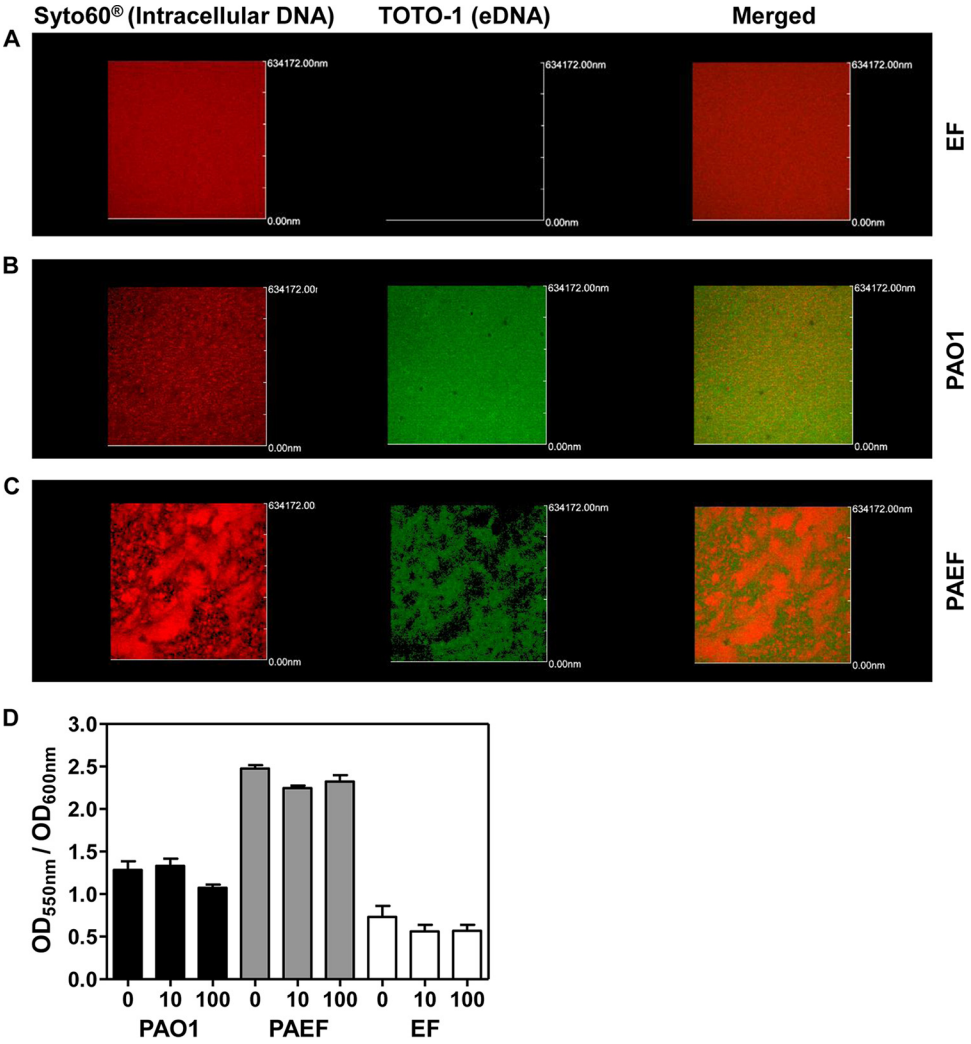

FIG 3 Extracellular DNA detection and DNase I treatment of mono- and dual-species *P. aeruginosa* and *E. faecalis* biofilms. The monospecies biofilms of *E. faecalis* (A), *P. aeruginosa* (B), and the dual-species biofilm of *E. faecalis* and *P. aeruginosa* (C) were stained for intracellular DNA (Syto60) and extracellular DNA (TOTO-1). Wavelengths of 652 nm and 514 nm were used for Syto60 and TOTO-1, respectively. (D) Crystal violet biofilm assay results when two different concentrations of DNase I (10 μg/ml and 100 μg/ml) were used to treat 32-h-old mature biofilms.

significant effect on the matrix thickening of the dual-species biofilm. Consistent with these results, dual-species biofilms did not exhibit any increase in alginate production (Fig. 4C). Alginate production was only slightly decreased in the PAO1 plus *E. faecalis* dual-species biofilm, compared with the PAO1 biofilm (Fig. 4C).

Other EPSs, Pel and Psl, are also known to be important for biofilm development for *P. aeruginosa* (28). Herein, Pel-negative PAO1 Δ*pelA* biofilm produced a similarly thicker phenotype relative to the PAO1 biofilm (Fig. 5A and Movie S4). In contrast, a Psl-negative Δ*psl* mutant strain showed no matrix thickness on its biofilm (Fig. 5B and Movie S6), demonstrating that Psl is critically involved in matrix thickening in PAO1 monospecies biofilm. The dual-species biofilm of the Δ*pelA* mutant plus *E. faecalis* showed a significantly increased biofilm matrix thickness, while the Δ*psl* mutant plus *E. faecalis* biofilm displayed a matrix thickness that recovered to normal levels (Fig. 5D and E, and Movies S5 and S7). These results suggest that the production of Psl and Pel is stimulated by the presence of *E. faecalis*. As expected, a PAO1 mutant defective in both Pel and Psl production, the Δ*pelA* Δ*psl* mutant, appeared to have no matrix thickness in both the mono- and dual-species biofilms (Fig. 5C and F, and Movies S8 and S9).

Psl stimulates intraspecies PAO1-PAO1 interactions, while Pel is involved in interspecies PAO1-*E. faecalis* interactions. Our results described above indicate that

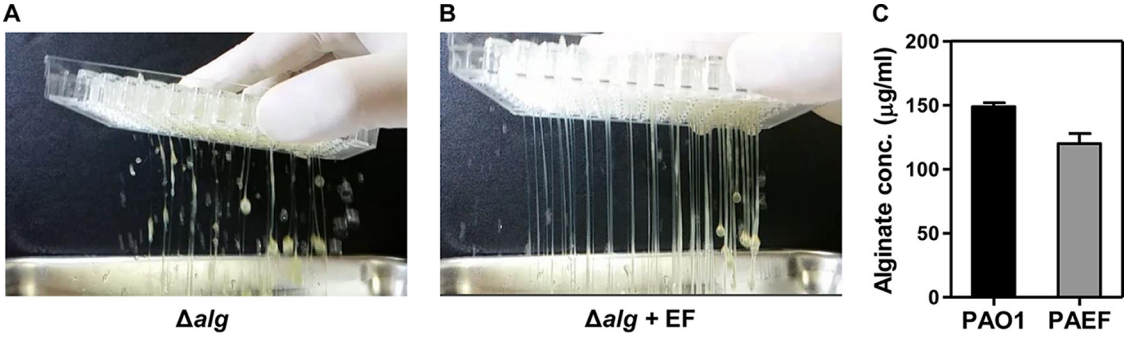

FIG 4 Alginate is not responsible for the elevated biofilm matrix thickness in the dual-species biofilms. The matrix thickness of biofilms was tested by flipping the biofilms upside down. Biofilms of PAO1 Δ*alg* mutant of its own (A) and with *E. faecalis* (B) were formed and tested. (C) Quantification of alginate production in PAO1 monospecies and PAO1 plus *E. faecalis* dual-species biofilms. *, $P < 0.05$ versus the alginate levels of PAO1 and PAO1 plus *E. faecalis* (PAEF).

both Psl and Pel are involved in matrix thickening in biofilms. Thus, we aimed to explore the effect of EPS deficiencies on the dual-species biofilm formation. The red fluorescent Δ*pelA* and Δ*psl* mutants presented with normal biofilm structures (Fig. 6A and B). The Δ*pelA* Δ*psl* double mutant, however, showed a dramatic decrease in its ability to produce biofilm (Fig. 6C). When each of these mutants was coculture with green fluorescent *E. faecalis*, different patterns of biofilm formation were observed. In the Δ*pelA* mutant plus *E. faecalis* dual-species biofilm, Δ*pelA* mutant cells and *E. faecalis* were spatially segregated, yielding a structurally distinct biofilm (Fig. 6D). Psl production appeared to be increased in the Δ*pelA* mutant plus *E. faecalis* dual-species biofilm (Fig. 5A and D), while Pel was absent in this particular biofilm. Thus, the results shown in Fig. 6D indicate that Psl is likely involved in PAO1-PAO1 intraspecies interactions. In contrast, the Δ*psl* mutant, when grown together with *E. faecalis*, produced a biofilm in which the two organisms were mixed quite evenly, suggesting that Pel is more involved in interspecies interactions between PAO1 and EF (Fig. 6E). The Δ*pelA* Δ*psl* mutant plus *E. faecalis* coculture biofilm presented with red fluorescent Δ*pelA* Δ*psl* mutant cells that were not detected in its own monospecies biofilm (Fig. 6C and F), suggesting that the biofilm-forming capability of the Δ*pelA* Δ*psl* mutant can be restored in the presence of EF, even though the biofilm still exhibited no matrix thickness, as demonstrated in

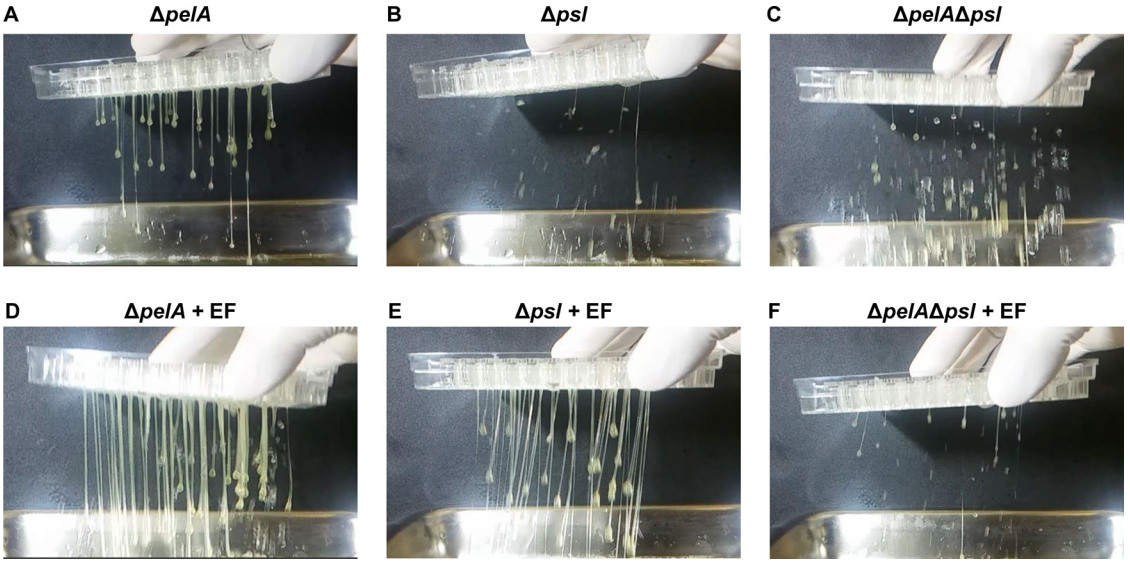

FIG 5 Role of Psl and Pel in the matrix thickening of the dual-species biofilms. The matrix thickness of biofilms was tested by flipping the biofilms upside down. PAO1 Δ*pelA* (A and D), Δ*psl* (B and E), and Δ*pelA* Δ*psl* mutants (C and F) were grown as monospecies biofilms (A to C) or together with EF (D to F) as dual-species biofilms.

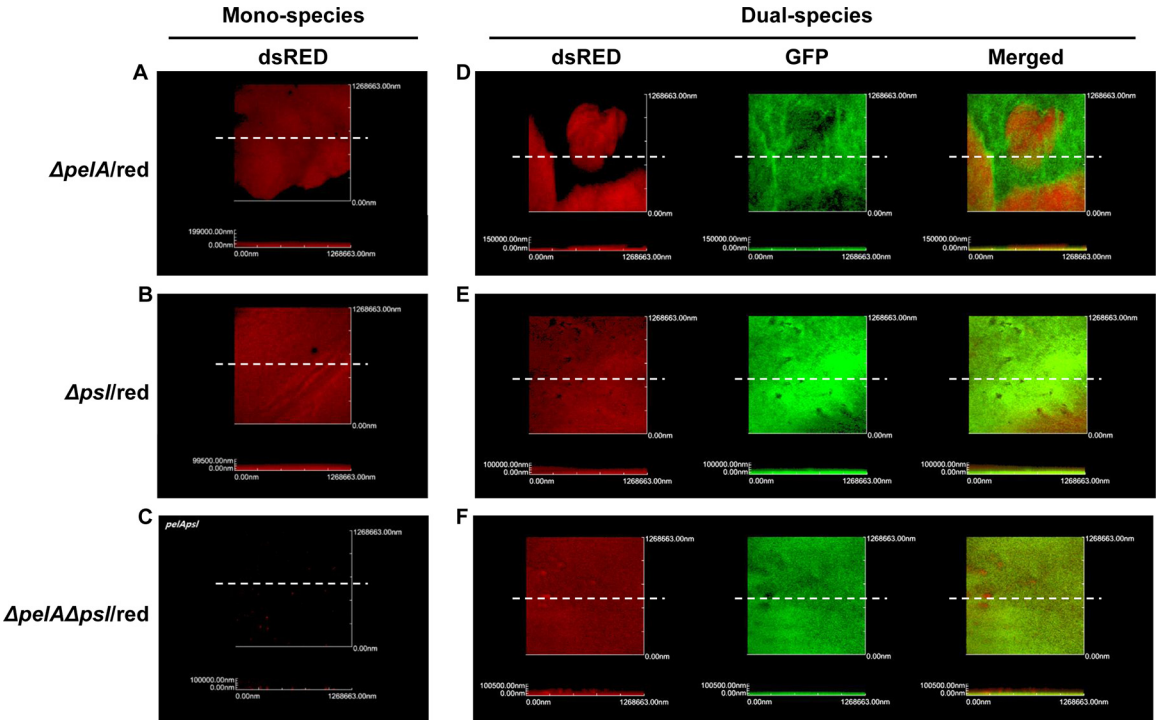

FIG 6 Biofilms of Δ*pelA*/red mutant, Δ*psl*/red mutant, and/or *EF*/green. The CLSM images of monospecies Δ*pelA*/red mutant (A), Δ*psl*/red mutant (B), Δ*pelA*Δ*psl*/red mutant (C), the dual-species *EF*/green and Δ*pelA*/red mutant (D), Δ*psl*/red mutant (E), and Δ*pelA*Δ*psl*/red mutant (F). White dotted lines indicate the locations of sagittal sections for height representation of the biofilms.

Fig. 5F. Together, these results suggest that Pel and Psl play distinct roles during the formation of dual-species biofilm.

qRT-PCR analysis of Psl and Pel production in mono- and dual-species biofilms. Quantitative real-time PCR (qRT-PCR) of *pslA* and *pelB* of the monospecies PAO1 biofilm and the dual-species biofilm was performed to quantify the expression levels of the two genes at different time points. The qRT-PCR data revealed that both *pslA* and *pelB* expression levels were increased in the dual-species biofilms (Fig. 7). The transcription levels of *pslA* were about 2-fold higher in the dual-species biofilm than in the PAO1 monospecies biofilm in the early and mature stages of biofilm development (Fig. 7A and B). The transcription levels of *pelB* were also higher in the dual-species biofilms than the monospecies biofilms (Fig. 7C and D). Interestingly, *pelB* was expressed much more in the early stage of biofilm development (approximately 30-fold that in the monospecies biofilm) than in the mature stage (approximately 6-fold that in the monospecies biofilm). The data confirm that Psl and Pel are expressed more in the dual-species biofilms and support the notion that Pel is closely related to interspecies interactions between *P. aeruginosa* and *E. faecalis*.

DISCUSSION

Most chronic infections have been shown to be associated with biofilm infections. However, the eradication of biofilm infections is still extremely difficult, and effective treatments other than surgical removal have not yet been found. One of the major reasons for the difficulties in biofilm infection treatment is that the majority of biofilm infections do not consist of a single bacterial species (13). Biofilms typically consist of multiple species of microbes, and the interactions between the microbes in biofilms make these biofilm infections more virulent and more resistant (10, 20, 29). In this investigation, we focused on characterizing and understanding a *P. aeruginosa* and *E. faecalis* dual-species biofilm, as the two species are some of the major causative agents of chronic biofilm infections (4, 20, 30).

P. aeruginosa and *E. faecalis* belong to two different bacterial groups, Gram-negative

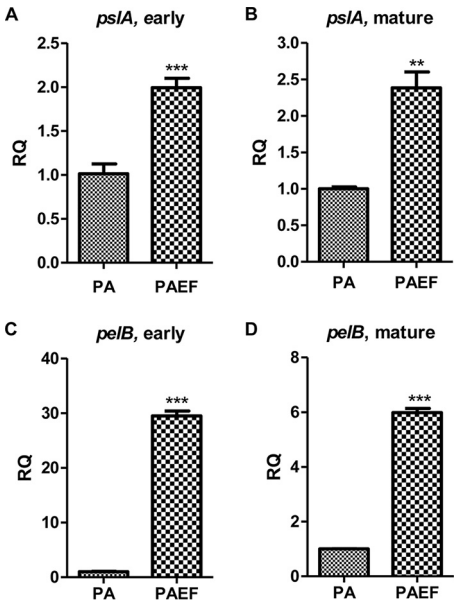

FIG 7 Quantitative real-time PCR analysis of *pslA* and *pelB* expression. The qRT-PCR of PAO1 monospecies (the reference samples; PA) and PAO1 plus *E. faecalis* dual-species (the experimental samples; PAEF) biofilms for *pslA* (A and B) and *pelB* (C and D) genes. Gene expression was measured at the early (A and C) and mature (B and D) stages of the biofilm developments. RQ represents the relative quantitation value for genetic expression. **, $P < 0.001$ versus gene expression of PAO1 and PAO1 plus *E. faecalis* biofilms. ***, $P < 0.0001$ versus gene expression of PAO1 and PAO1 plus *E. faecalis* biofilms.

and Gram-positive bacteria, respectively, and they cause biofilm infections in similar areas of the human body, such as the urinary tract and wounds (8, 11, 21, 30, 31). Preliminary experiments on the coculturability of *P. aeruginosa* and *E. faecalis* showed that *P. aeruginosa* and *E. faecalis* did not affect each other's growth under planktonic culture conditions (Fig. 1B and C). Interestingly, the CV biofilm assay showed enhanced biofilm formation (Fig. 1D), and biofilm matrix thickness was enhanced substantially in the dual-species biofilm compared to the monospecies biofilms (Fig. 1E and the movies in the supplemental material). SEM images of the biofilms indicated that there was increased production in the ECM in the dual-species biofilm (Fig. 1F). According to these observations, we discerned that these two bacterial species interact with each other and have synergistic effects on biofilm development.

In our investigation, the dual-species biofilm presented with a more structured PAO1/red biofilm than the monospecies biofilm on top of a flat *EF*/green biofilm layer (Fig. 2). This spatial distribution of the dual-species biofilm might be due to the ability to grow under a lack of oxygen. Even though both bacterial species are facultative anaerobes, *E. faecalis* is able to grow using fermentation pathways, while *P. aeruginosa* cannot ferment and requires nitrogen oxides as an alternative electron acceptor for anaerobic growth (18, 32). Therefore, it would be more efficient for *P. aeruginosa* to reside on top of *E. faecalis* in the dual-species biofilm, as there is more oxygen available. The dual-species biofilms were prepared with a 24-h interval between the inoculation times of each bacterium. Regardless of which bacterial species was inoculated first, the biofilms presented the same spatial distribution (data not shown).

One of the major components of the ECM is eDNA, which is known to play a role in the adhesion of bacterial cells on surfaces with repulsive electronic charge and structure stability (24, 25). Accordingly, we observed eDNA in the mono- and dual-species *P. aeruginosa* and *E. faecalis* biofilms. The *E. faecalis* biofilm presented no eDNA (Fig. 3A). On the other hand, the *P. aeruginosa* biofilm was covered with a substantial amount of eDNA (Fig. 3B). Notwithstanding, the production and distribution of eDNA in the dual-species biofilm were not exactly as we expected: first, the amount of eDNA was not increased in the dual-species biofilm compared to that in the *P. aeruginosa*

monospecies biofilm (Fig. 3C). Second, the distribution of eDNA in the dual-species biofilm was mainly present outside structured biofilms, which may indicate that the eDNA acts less in biofilm structure formation of *P. aeruginosa* and that the eDNA was present due to the *P. aeruginosa*. Furthermore, regardless of when and how much DNase I was used, it did not significantly affect the dual-species biofilm (Fig. 3D). According to these results, we deduced that eDNA is not an essential component of the ECM in dual-species biofilm formation.

Another major component of the ECM is EPS. Herein, *P. aeruginosa* mutants defective in the production of each known EPS molecule, alginate, Pel, and Psl, were constructed, and matrix thickening of the biofilms with these mutants and *E. faecalis* was observed (Fig. 4 and 5, and the movies in the supplemental material). In biofilms of each *P. aeruginosa* EPS gene knockout, alginate and Psl seemed to be necessary to obtain thickening of the matrix of the *P. aeruginosa* biofilm; however, the Δ*pelA* Δ*psl* mutant biofilm showed that alginate alone did not express the matrix thickening of *P. aeruginosa* biofilms (Fig. 5C and Movie S8). The Δ*pelA* Δ*psl* mutant plus *E. faecalis* biofilm showed that alginate is not significantly involved in interspecies interactions with *E. faecalis* for matrix thickening (Fig. 5F and Movie S9). The Δ*alg* mutant plus *E. faecalis* biofilm results indicated that both Pel and Psl are necessary for increased matrix thickness (Fig. 4B). Meanwhile, the Δ*pelA* mutant plus *E. faecalis* and Δ*psl* mutant plus *E. faecalis* biofilms showed that Psl is associated more with the matrix thickness of monospecies biofilm and bacterial surface adhesion and that Pel is more related to interspecies interactions, since the matrix thickness of the Δ*psl* mutant plus *E. faecalis* biofilm recovered to normal levels (Fig. 5E and Movie S7). Even though alginate did not seem to be directly involved in matrix thickening, alginate is known to be an important factor for virulence and antibiotic resistance in *P. aeruginosa* biofilms (33, 34). Therefore, we evaluated alginate production in the mono- and dual-species biofilms via the alginate assay. The results showed no enhancement of alginate in the dual-species biofilm (Fig. 4).

The CLSM images of The PAO1 Δ*pelA* mutant exhibiting red fluorescence (Δ*pelA/*red) and PAO1 Δ*psl* mutant exhibiting red fluorescence (Δ*psl/*red) with *EF/*green biofilms indicated that Psl is involved in the interaction between *P. aeruginosa* cells to form a structured biofilm and that Pel has a greater role in interspecies interactions (Fig. 6). The data also confirmed that *P. aeruginosa* loses the ability to form biofilm when both Pel and Psl are missing (Fig. 6C). However, the Δ*pelA* Δ*psl* mutant plus *E. faecalis* biofilm showed that Δ*pelA* Δ*psl/*red exists within the *EF/*green biofilm, indicating that *E. faecalis* has the ability to weakly interact with *P. aeruginosa* (Fig. 6F). Nevertheless, Δ*pelA* Δ*psl* mutant plus *E. faecalis* biofilm did not present any matrix thickness, suggesting that the matrix thickening of the dual-species biofilm is solely due to Pel and Psl (Fig. 5). qRT-PCR analysis also revealed increased production of Psl and Pel in the dual-species biofilms (Fig. 7). The significant increase in Pel production might indicate that Pel plays an important role in the interspecies interaction of *P. aeruginosa* and *E. faecalis*. A limitation of the study, however, was that it was difficult to distinguish between Pel, Psl, and alginate in these biofilms. Different approaches are needed to precisely distinguish the distribution of each EPS. Furthermore, Chew et al. reported similar results for a *P. aeruginosa* and *S. aureus* mixed biofilm (35). This may suggest that the results that we obtained reflect general characteristics of *P. aeruginosa* and Gram-positive coccus mixed biofilms.

In conclusion, *P. aeruginosa* and *E. faecalis* can form a dual-species biofilm and have a distinct spatial distribution within the biofilm. *E. faecalis* tends to locate at the bottom of the biofilm, and *P. aeruginosa* forms a more structured biofilm on the top of the *E. faecalis* biofilm. However, the species were not completely separated, as the biofilms did contain cells of the other species when observed under higher magnifications (data not shown). The dual-species biofilm had much thicker ECM than its monospecies counterparts, potentially contributing to the increase in virulence of polymicrobial biofilm infections. For examples, the thicker ECM can protect the dual-species biofilms from antimicrobial reagents, host immune responses, and other environmental stresses.

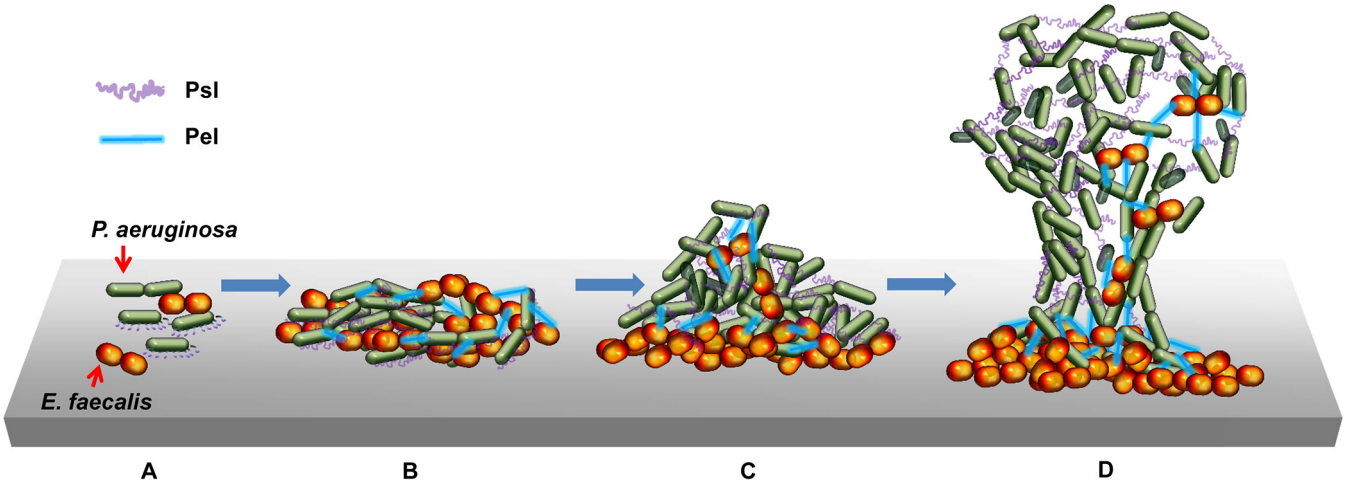

FIG 8 Scheme of the dual-species *P. aeruginosa* and *E. faecalis* biofilm development. (A) *P. aeruginosa* and *E. faecalis* attach to a surface without spatial separation. (B) During the early stages of dual-species biofilm formation, the attached cells proliferate and start producing EPS, Pel (blue straight line), and Psl (purple curved line). (C) *P. aeruginosa* and *E. faecalis* start to exhibit distinct spatial distributions. (D) In the maturation stage of the dual-species biofilm, *P. aeruginosa* forms a structured biofilm on top of the *E. faecalis* biofilm: Psl is associated with the surface and between *P. aeruginosa*, while Pel is associated with interspecies interactions between *P. aeruginosa* and *E. faecalis*.

The Psl polysaccharide can inhibit opsonization, which resulted in a decrease in reactive oxygen species (ROS) production by neutrophils (36). As a result of the increased ECM, the biofilm infection can become chronic. This phenotype was mainly due to components of the ECM, particularly Pel and Psl, rather than eDNA and alginate (Fig. 8). Therefore, targeting Pel and Psl of *P. aeruginosa* might help eradicate polymicrobial infections more effectively. Furthermore, the results of biofilm formation experiments with supernatants or fixed cells of *E. faecalis* under planktonic or static culture conditions indicated that cell-to-cell contact with live *E. faecalis* is essential for the expression of the thicker matrix phenotype of the dual-species biofilm (data not shown). This indicates that there should be a mechanism for live *E. faecalis* recognition on the *P. aeruginosa* membrane, and the identification of said mechanism will likely contribute to the development of a method with which to eradicate polymicrobial biofilms with *P. aeruginosa*. Further investigation of the matrix-thickening factors of the dual-species biofilm with *E. faecalis* is warranted. Investigation using *E. faecalis* forward genetic screening is in progress.

MATERIALS AND METHODS

Bacterial strains and growth conditions. *P. aeruginosa* and *E. faecalis* were used as the model bacteria for this polymicrobial biofilm study. *P. aeruginosa* PAO1 (wild type) was used as the basis for all mutant *P. aeruginosa* strains used in this investigation. *E. faecalis* 12448 (Korean Culture Collection of Microorganism [KCCM]) was used for nonfluorescent *E. faecalis* experiments. *E. faecalis* OG1RF harboring pMV158GFP (*EF*/green) and pAMβ1 were used for the fluorescent *E. faecalis* experiments. *P. aeruginosa* harboring the pME plasmid vector that was transcriptionally fused with a dsRED gene after GFP promoter (pME-dsRED) was constructed in the lab (PAO1/red). The *E. faecalis* pMV158GFP plasmid possessed a tetracycline resistance (Tet^r) marker, and *P. aeruginosa* pME-dsRED contained a gentamicin resistance (Gm^r) marker. The bacterial strains and plasmids used are described in Table 1. *P. aeruginosa* strains lacking plasmid were grown in Luria-Bertani (LB) medium at 37°C. For selection purposes, *P. aeruginosa* harboring pME-dsRED (PAO1/red) was grown on LB medium with 100 μg/ml gentamicin. *E. faecalis* was grown on brain heart infusion broth (BHIB) medium, and *E. faecalis* pMV158GFP (*EF*/green) was grown on BHIB medium with tetracycline (1 μg/ml) and erythromycin (1 μg/ml) to maintain the plasmids.

Construction of the *alg*, *pelA*, *psl*, and *pelA psl* clean-deletion mutants. The Δ*alg*, Δ*pelA*, Δ*psl*, and Δ*pelA* Δ*psl* mutants were constructed by allelic replacement (37). Briefly, approximately 600 bp of flanking sequences at both ends of each gene or operon were amplified by PCR with primers (Table 2). The upstream reverse primers and the downstream forward primers were complementary to each other. Thus, the 3′ end of the upstream sequence and the 5′ end of the downstream sequence were annealed together during PCR amplification. The Δ*pelA* Δ*psl* double mutant was constructed by performing the allelic replacement twice. The deletions of the *alg*, *pelA*, and *psl* operon genes were confirmed by PCR and DNA sequencing.

TABLE 1 Bacterial strains and plasmids used in this investigation

Strain or plasmid	Description[a]	Reference or source
Bacterial strains		
PAO1	Prototype *P. aeruginosa* laboratory strain	ATCC 10145
Δ*alg* mutant	PAO1 with in-frame deletion of *alg* operon (PA3540–PA3548)	This study
Δ*pelA* mutant	PAO1 with in-frame deletion of PA3064 gene	This study
Δ*psl* mutant	PAO1 with in-frame deletion of *psl* operon (PA2231–PA2242)	This study
Δ*pelA* Δ*psl* mutant	PAO1 with in-frame deletion of PA3064 gene and *psl* operon	This study
PAO1/red	PAO1 harboring pME-dsRED	This study
Δ*alg*/red	Δ*alg* mutant harboring pME-dsRED	This study
Δ*pelA*/red	Δ*pelA* mutant harboring pME-dsRED	This study
Δ*psl*/red	Δ*psl* mutant harboring pME-dsRED	This study
Δ*pelA* Δ*psl*/red	Δ*pelA* Δ*psl* mutant harboring pME-dsRED	This study
E. faecalis 12448	*E. faecalis* type strain (ATCC 19433)	Korean Culture Collection of Microorganisms (KCCM)
EF/green	*E. faecalis* OG1RF strain, harboring pMV158GFP and pAMβ1	41
Plasmids		
pME-dsRED	Transcriptional fusion of GFP promoter with a gene encoding DsRed, Gm^r	This study
pMV158GFP	pMV158, harbors the GFP gene under the control of the P_M-inducible promoter, Tet^r	41
pAMβ1	Auxiliary plasmid for pMV158GFP transport, Em^r	41

[a]GFP, green fluorescent protein; Gm^r, gentamicin resistance; Tet^r, tetracycline resistance; Em^r, erythromycin resistance.

Biofilm preparation. Biofilms were prepared in accordance with the method described by O'Toole (38). Briefly, a static biofilm was prepared by inoculating subcultured bacterial strains (1:100 dilution) in BHIB. BHIB was used for both *P. aeruginosa* strain and *E. faecalis* strain biofilms: *E. faecalis* strains presented retarded growth in LB medium, whereas *P. aeruginosa* showed similar growth in LB and BHIB media (data not shown). Biofilms for quantification and visual observation were prepared in 96-well plates (HM, South Korea), biofilms for confocal microscopy were prepared in glass-bottom confocal dishes (SPL, South Korea), and biofilms for matrix thickness measurement and extracellular matrix analysis were prepared in 500-ml cell culture flasks (SPL).

Biofilm analysis. The quantification of biofilms was executed by crystal violet (CV) biofilm assays (38). Also, the CFU of biofilms were measured. The biofilms, grown in 96-well plates, were sonicated with three 10-s pulses at 40 kHz (Branson 8510 ultrasonic cleaner) to disperse the biofilm-associated bacterial cells. Sonicated biofilm samples (100 μl) were harvested and serially diluted for CFU measurements.

Matrix thickness measurements. Observations by the naked eye were made to assess the matrix thickening of each biofilm. Biofilms were grown in 96-well plates for 48 h and dumped by turning the plates upside down. The thicknesses of biofilms and their ECMs were observed. Briefly, 50 ml of the biofilm was grown in a 500-ml cell culture flask for 48 h at 37°C. Then, the medium was carefully removed by pipetting and rinsing the biofilms with phosphate-buffered saline (PBS) once to remove planktonic cells. The biofilms and their matrices from the surface of the cell culture flask were harvested using cell scrapers. The harvested biofilms and ECMs were transferred to 50-ml conical tubes (HM, South Korea), and viscosity was measured using a viscometer (Brookfield digital viscometer model DV-II) with spindle no. 6 (RV/HA/HB series) at 25°C and 50 rpm. The viscosity measurements were performed three times for each biofilm sample, and average readings thereof were recorded.

CLSM image analysis of biofilms. Differential interference contrast (DIC) images were acquired using a confocal laser scanning microscope (FV-1000; Olympus Optical Co. Ltd., Japan) equipped with FV10-ASW operating software (version 02.01). For CLSM image analysis, biofilms were grown in cover-glass bottom dishes (SPL, South Korea). After 24 h of biofilm growth, the planktonic portion of the cultures was removed, and the plates were washed with 0.9% saline. Bacterial strains harboring fluorescent plasmids were examined at 488 nm and 594 nm for the pMV158GFP and pME-dsRED plasmids, respectively. Syto60 (Life Technologies) and TOTO-1 (Life Technologies) fluorescent dyes were used for the detection of intracellular DNA and extracellular DNA, respectively. Excitation wavelengths at 652 nm and 514 nm were used for Syto60 and TOTO-1, respectively. Calcofluor white dye was used for EPS detection at 358 nm. For three-dimensional (3D) image analysis, Z-stack images were obtained, and 3D images were reconstructed using the FV10-ASW software. The ImageJ program was used to analyze the fluorescence intensities of the Z-stack images (39).

SEM of biofilms. The biofilm samples were grown on 12-mm round cover glass and fixed with Karnovsky fixing solution (2% glutaraldehyde, 2% paraformaldehyde, 0.5% $CaCl_2$) for 6 h. The fixed samples were washed with 0.1 M phosphate buffer for 2 h and treated with 1% OsO_4 for 2 h. Then, the biofilm samples were dehydrated in an ascending gradual series (50 to ~100%) of ethanol, infiltrated with isoamyl acetate, and dried (critical point dryer HCP-2; Hitachi, Japan). The dried biofilm samples were coated with gold via ion sputter at 6 mA for 6 min. The samples were observed using field emission scanning electron microscopy (FE-SEM; S-800; Hitachi Ltd., Tokyo, Japan).

Alginate quantification. Bacterial alginate was indirectly quantified by means of an alginate assay that measures uronic acid levels using a D-mannuronic acid lactone standard curve (40). Briefly, bacterial samples were grown at 37°C for 24 h in both planktonic and biofilm modes of growth. The planktonic cultures were centrifuged to obtain supernatants. The supernatants of the biofilm samples were carefully

TABLE 2 Primers used in this study

Mutation/gene target by primer type	Flanking region	Direction	Primer sequence (5′–3′)[a]	Restriction enzyme
Primers for clean deletion				
alg	Left	Forward	ACCTTGAGCTCGCATGGGTCGAAGATTAAGG	SacI
	Left	Reverse	CGTTAATGAGGTGGCCGTATAAGTCGAAGTAGAGCTGCGC	
	Right	Forward	GCGCAGCTCTACTTCGACTTATACGGCCACCTCATTAACG	
	Right	Reverse	TAGAGGAGCTCTCTGCAATGGCTGGTTGTAG	SacI
psl	Left	Forward	ACCTTGCATGCGGGCTGGTACATCCAGAAGA	SphI
	Left	Reverse	TCGTCGATAGTGGCTTTGTGAGCATTCCGACAAGGAGC	
	Right	Forward	GCTCCTTGTCGGAATGCTCACAAAGCCACTATCGACGA	
	Right	Reverse	TAGAGGCATGCGCATCGACCTGAAAATCCTC	SphI
pelA	Left	Forward	ACCTTGAGCTCCGATCATCCTCGGCTTTCT	SacI
	Left	Reverse	CAAAACCTGTCGCGTAGTGGTAATCGCTCATCCACAGC	
	Right	Forward	GCTGTGGATGAGCGATTACCACTACGCGACAGGTTTTG	
	Right	Reverse	TAGAGGAGCTCCGCTGGGCATGAATACTTCT	SacI
qRT-PCR primers				
pelA		Forward	GGT GAT TAT GTT CCA GGC ACT	
		Reverse	GGT GAA CCA GAA GAT CAC CA	
pslB		Forward	TGG CTG ACC TTC AAC AGC GA	
		Reverse	TGC TCG AAG TCA CCG AGC TT	
16S rRNA		Forward	CTT ACG GCC AGG GCT ACA CA	
		Reverse	GTA CAA GGC CCG GGA ACG TA	

[a]Restriction enzyme recognition sites are underlined.

harvested by pipetting, and the remaining biofilms were scraped for harvesting. The biofilm samples were sonicated, and the resultant supernatants were harvested. The culture supernatants (20 μl) were mixed with 80 μl of distilled water and assayed for alginate quantification (40). One hundred microliters each of alginate standard and sample were mixed thoroughly with 600 μl of the cold sulfuric acid-borate solution in an ice bath. The mixtures were heated to 100°C for 10 min and then rapidly cooled in an ice bath. Ten microliters of 0.1% carbazole solution was added to the mixture and reheated at 100°C for 15 min. The samples were cooled immediately in ice after heating. The absorbance at 525 nm was measured. The optical density at 600 nm (OD_{600}) values of bacterial suspensions were used for normalization.

qRT-PCR analysis of Pel and Psl production in monospecies and dual-species biofilms. Pel and Psl polysaccharide production was indirectly measured by qRT-PCR analysis of *pslA* and *pelB*, the constituents of the *psl* and *pel* operons, respectively. The primer sequences used for the qRT-PCR are listed in Table 2. Briefly, PAO1 monospecies biofilms and PAO1 plus *E. faecalis* dual-species biofilms were harvested at 4 h and 24 h postinoculation. RNA was isolated using an RNeasy minikit (Qiagen). cDNA was prepared using the PrimeScript II first-strand cDNA synthesis kit (TaKaRa Bio, Inc., Japan). qRT-PCR was performed using a SYBR Premix *Ex Taq* kit (TaKaRa Bio, Inc.) and gene-specific primers. For each sample, three qRT-PCR replicates were performed using the Applied Biosystems 7300 real-time PCR system. The following thermocycling conditions were utilized: 94°C for 5 min, followed by 40 cycles of 94°C for 30 s, 60°C for 30 s, and 72°C for 1 min. The level of each gene was normalized to that of the 16S rRNA of *P. aeruginosa*. The results are expressed relative to the gene expression level obtained with gene-specific primers from the PAO1 monospecies biofilm.

Statistical analysis. All data are expressed as the mean ± standard deviation (SD). Unpaired Student's *t* test and one-way analysis of variance (ANOVA) were used to analyze the significance of all comparisons. A P value of <0.05 was considered statistically significant. All experiments were repeated at least three times for reproducibility.

SUPPLEMENTAL MATERIAL

Supplemental material for this article may be found at https://doi.org/10.1128/AEM.01182-17.

SUPPLEMENTAL FILE 1, PDF file, 0.4 MB.
SUPPLEMENTAL FILE 2, MP4 file, 2.2 MB.
SUPPLEMENTAL FILE 3, MP4 file, 1.1 MB.
SUPPLEMENTAL FILE 4, MP4 file, 1.2 MB.
SUPPLEMENTAL FILE 5, MP4 file, 1.3 MB.
SUPPLEMENTAL FILE 6, MP4 file, 2.0 MB.
SUPPLEMENTAL FILE 7, MP4 file, 0.8 MB.
SUPPLEMENTAL FILE 8, MP4 file, 1.1 MB.
SUPPLEMENTAL FILE 9, MP4 file, 1.2 MB.
SUPPLEMENTAL FILE 10, MP4 file, 1.0 MB.

ACKNOWLEDGMENTS

E. faecalis OG1RF harboring pMV158GFP (*EF*/green) and pAMβ1 was kindly provided by Manuel Espinosa Padron (Centro de Investigaciones Biológicas, Consejo Superior de Investigaciones Científicas, Madrid, Spain).

This work was supported by grants from the National Research Foundation of Korea (NRF), funded by the South Korean government (grants 2014R1A2A2A01002861 and 2014R1A4A1008625). This work was also supported by a grant from the Korea Healthcare Technology R&D project, of the Ministry of Health, Welfare, and Family Affairs (grant HI15C0694).

REFERENCES

1. O'Toole G, Kaplan HB, Kolter R. 2000. Biofilm formation as microbial development. Annu Rev Microbiol 2000 54:49–79.
2. Hall-Stoodley L, Costerton JW, Stoodley P. 2004. Bacterial biofilms: from the natural environment to infectious diseases. Nat Rev Microbiol 2:95–108. https://doi.org/10.1038/nrmicro821.
3. Costerton JW, Stewart PS, Greenberg EP. 1999. Bacterial biofilms: a common cause of persistent infections. Science 21:1318–1322. https://doi.org/10.1126/science.284.5418.1318.
4. Clinton A, Carter T. 2015. Chronic wound biofilms: pathogenesis and potential therapies. Lab Med 46:277–284. https://doi.org/10.1309/LMBNSWKUI4JPN7SO.
5. Donlan RM. 2001. Biofilms and device-associated infections. Emerg Infect Dis 7:277–281. https://doi.org/10.3201/eid0702.010226.
6. Sandoe JA, Witherden IR, Cove JH, Heritage J, Wilcox MH. 2003. Correlation between enterococcal biofilm formation *in vitro* and medical-device-related infection potential *in vivo*. J Med Microbiol 52:547–550. https://doi.org/10.1099/jmm.0.05201-0.
7. Lleo M, Bonato B, Tafi MC, Caburlotto G, Benedetti D, Canepari P. 2007. Adhesion to medical device materials and biofilm formation capability of some species of enterococci in different physiological states. FEMS Microbiol Lett 274:232–237. https://doi.org/10.1111/j.1574-6968.2007.00836.x.
8. Niveditha S, Pramodhini S, Umadevi S, Kumar S, Stephen S. 2012. The isolation and the biofilm formation of uropathogens in the patients with catheter-associated urinary tract infections (UTIs). J Clin Diagn Res 6:1478–1482.
9. Fernandes A, Dias M. 2013. The microbiological profiles of infected prosthetic implants with an emphasis on the organisms which form biofilms. J Clin Diagn Res 7:219–223.
10. Wolcott R, Costerton JW, Raoult D, Cutler SJ. 2013. The polymicrobial nature of biofilm infection. Clin Microbiol Infect 19:107–112. https://doi.org/10.1111/j.1469-0691.2012.04001.x.
11. Semedo-Lemsaddek T, Mottola C, Alves-Barroco C, Cavaco-Silva P, Tavares L, Oliveira M. 2016. Characterization of multidrug-resistant diabetic foot ulcer enterococci. Enferm Infecc Microbiol Clin 34:114–116. https://doi.org/10.1016/j.eimc.2015.01.007.
12. Burmølle M, Thomsen TR, Fazli M, Dige I, Christensen L, Homoe P, Tvede M, Nyvad B, Tolker-Nielsen T, Givskov M, Moser C, Kirketerp-Moller K, Johansen HK, Hoiby N, Jensen PO, Sorensen SJ, Bjarnsholt T. 2010. Biofilms in chronic infections–a matter of opportunity–monospecies biofilms in multispecies infections. FEMS Immunol Med Microbiol 59:324–336. https://doi.org/10.1111/j.1574-695X.2010.00714.x.
13. Peters BM, Jabra-Rizk MA, O'May GA, Costerton JW, Shirtliff ME. 2012. Polymicrobial interactions: impact on pathogenesis and human disease. Clin Microbiol Rev 25:193–213. https://doi.org/10.1128/CMR.00013-11.
14. Harriott MM, Noverr MC. 2009. *Candida albicans* and *Staphylococcus aureus* form polymicrobial biofilms: effects on antimicrobial resistance. Antimicrob Agents Chemother 53:3914–3922. https://doi.org/10.1128/AAC.00657-09.
15. Colombo AV, Barbosa GM, Higashi D, di Micheli G, Rodrigues PH, Simionato MR. 2013. Quantitative detection of *Staphylococcus aureus*, *Enterococcus faecalis* and *Pseudomonas aeruginosa* in human oral epithelial cells from subjects with periodontitis and periodontal health. J Med Microbiol 62:1592–1600. https://doi.org/10.1099/jmm.0.055830-0.
16. Korgaonkar A, Trivedi U, Rumbaugh KP, Whiteley M. 2013. Community surveillance enhances *Pseudomonas aeruginosa* virulence during polymicrobial infection. Proc Natl Acad Sci U S A 110:1059–1064. https://doi.org/10.1073/pnas.1214550110.
17. Alhazmi A. 2015. *Pseudomonas aeruginosa*—pathogenesis and pathogenic mechanisms. Int J Biol 7:44–67. https://doi.org/10.5539/ijb.v7n2p44.
18. Fisher K, Phillips C. 2009. The ecology, epidemiology and virulence of *Enterococcus*. Microbiology 155:1749–1757. https://doi.org/10.1099/mic.0.026385-0.
19. Nallapareddy SR, Singh KV, Sillanpaa J, Garsin DA, Hook M, Erlandsen SL, Murray BE. 2006. Endocarditis and biofilm-associated pili of *Enterococcus faecalis*. J Clin Invest 116:2799–2807. https://doi.org/10.1172/JCI29021.
20. Dowd SE, Wolcott RD, Sun Y, McKeehan T, Smith E, Rhoads D. 2008. Polymicrobial nature of chronic diabetic foot ulcer biofilm infections determined using bacterial tag encoded FLX amplicon pyrosequencing (bTEFAP). PLoS One 3:e3326. https://doi.org/10.1371/journal.pone.0003326.
21. Mohamed JA, Huang DB. 2007. Biofilm formation by enterococci. J Med Microbiol 56:1581–1588. https://doi.org/10.1099/jmm.0.47331-0.
22. Korgaonkar AK, Whiteley M. 2011. *Pseudomonas aeruginosa* enhances production of an antimicrobial in response to *N*-acetylglucosamine and peptidoglycan. J Bacteriol 193:909–917. https://doi.org/10.1128/JB.01175-10.
23. Tsuchimori N, Hayashi R, Shino A, Yamazaki T, Okonogi K. 1994. *Enterococcus faecalis* aggravates pyelonephritis caused by *Pseudomonas aeruginosa* in experimental ascending mixed urinary tract infection in mice. Infect Immun 62:4534–4541.
24. Whitchurch CB, Tolker-Nielsen T, Ragas PC, Mattick JS. 2002. Extracellular DNA required for bacterial biofilm formation. Science 295:1487. https://doi.org/10.1126/science.295.5559.1487.
25. Okshevsky M, Meyer RL. 2015. The role of extracellular DNA in the establishment, maintenance and perpetuation of bacterial biofilms. Crit Rev Microbiol 41:341–352. https://doi.org/10.3109/1040841X.2013.841639.
26. Yoon SS, Coakley R, Lau GW, Lymar SV, Gaston B, Karabulut AC, Hennigan RF, Hwang SH, Buettner G, Schurr MJ, Mortensen JE, Burns JL, Speert D, Boucher RC, Hassett DJ. 2006. Anaerobic killing of mucoid *Pseudomonas aeruginosa* by acidified nitrite derivatives under cystic fibrosis airway conditions. J Clin Invest 116:436–446. https://doi.org/10.1172/JCI24684.
27. Wozniak DJ, Wyckoff TJ, Starkey M, Keyser R, Azadi P, O'Toole GA, Parsek MR. 2003. Alginate is not a significant component of the extracellular polysaccharide matrix of PA14 and PAO1 *Pseudomonas aeruginosa* biofilms. Proc Natl Acad Sci U S A 100:7907–7912. https://doi.org/10.1073/pnas.1231792100.
28. Colvin KM, Gordon VD, Murakami K, Borlee BR, Wozniak DJ, Wong GC, Parsek MR. 2011. The Pel polysaccharide can serve a structural and protective role in the biofilm matrix of *Pseudomonas aeruginosa*. PLoS Pathog 7:e1001264. https://doi.org/10.1371/journal.ppat.1001264.
29. Roy S, Elgharably H, Sinha M, Ganesh K, Chaney S, Mann E, Miller C, Khanna S, Bergdall VK, Powell HM, Cook CH, Gordillo GM, Wozniak DJ, Sen CK. 2014. Mixed-species biofilm compromises wound healing by disrupting epidermal barrier function. J Pathol 233:331–343. https://doi.org/10.1002/path.4360.
30. Watters C, DeLeon K, Trivedi U, Griswold JA, Lyte M, Hampel KJ, Wargo MJ, Rumbaugh KP. 2013. *Pseudomonas aeruginosa* biofilms perturb wound resolution and antibiotic tolerance in diabetic mice. Med Microbiol Immunol 202:131–141. https://doi.org/10.1007/s00430-012-0277-7.
31. Watters C, Everett JA, Haley C, Clinton A, Rumbaugh KP. 2014. Insulin treatment modulates the host immune system to enhance *Pseudomonas aeruginosa* wound biofilms. Infect Immun 82:92–100. https://doi.org/10.1128/IAI.00651-13.
32. Sharma G, Rao S, Bansal A, Dang S, Gupta S, Gabrani R. 2014. *Pseudomonas aeruginosa* biofilm: potential therapeutic targets. Biologicals 42:1–7. https://doi.org/10.1016/j.biologicals.2013.11.001.

33. Min KB, Lee KM, Oh YT, Yoon SS. 2014. Nonmucoid conversion of mucoid *Pseudomonas aeruginosa* induced by sulfate-stimulated growth. FEMS Microbiol Lett 360:157–166. https://doi.org/10.1111/1574-6968.12600.
34. Høiby N, Bjarnsholt T, Givskov M, Molin S, Ciofu O. 2010. Antibiotic resistance of bacterial biofilms. Int J Antimicrob Agents 35:322–332. https://doi.org/10.1016/j.ijantimicag.2009.12.011.
35. Chew SC, Kundukad B, Seviour T, van der Maarel JR, Yang L, Rice SA, Doyle P, Kjelleberg S. 2014. Dynamic remodeling of microbial biofilms by functionally distinct exopolysaccharides. mBio 5(4):e01536-14. https://doi.org/10.1128/mBio.01536-14.
36. Mishra M, Byrd MS, Sergeant S, Azad AK, Parsek MR, McPhail L, Schlesinger LS, Wozniak DJ. 2012. *Pseudomonas aeruginosa* Psl polysaccharide reduces neutrophil phagocytosis and the oxidative response by limiting complement-mediated opsonization. Cell Microbiol 14:95–106. https://doi.org/10.1111/j.1462-5822.2011.01704.x.
37. Lee KM, Park Y, Bari W, Yoon MY, Go J, Kim SC, Lee HI, Yoon SS. 2012. Activation of cholera toxin production by anaerobic respiration of trimethylamine *N*-oxide in *Vibrio cholerae*. J Biol Chem 287:39742–39752. https://doi.org/10.1074/jbc.M112.394932.
38. O'Toole GA. 2011. Microtiter dish biofilm formation assay. J Vis Exp 2011(47):e2437. https://doi.org/10.3791/2437.
39. Abramoff MD, Magalhaes PJ, Ram SJ. 2004. Image processing with ImageJ. Biophotonics Int 11:36–42.
40. Damron FH, Qiu D, Yu HD. 2009. The *Pseudomonas aeruginosa* sensor kinase KinB negatively controls alginate production through AlgW-dependent MucA proteolysis. J Bacteriol 191:2285–2295. https://doi.org/10.1128/JB.01490-08.
41. Nieto C, Espinosa M. 2003. Construction of the mobilizable plasmid pMV158GFP, a derivative of pMV158 that carries the gene encoding the green fluorescent protein. Plasmid 49:281–285. https://doi.org/10.1016/S0147-619X(03)00020-9.